Creep Crack Growth in a Type 316 Stainless Steel Weld Metal

Creep cracking can best be avoided by postweld heat treatment, by keeping delta ferrite below about 4% or by depositing small weld beads

BY J. R. HAIGH

ABSTRACT. Creep crack growth tests were performed on an AISI Type 316 stainless steel weld metal at 538 C (1000 F) using deeply cracked specimens subjected to bending moments. Results are expressed in terms of crack opening displacements and aspect ratios of the cracks because stress based methods commonly used are not applicable to the 316 weld metal. The steel was unusually brittle for Type 316 because δ-ferrite provided a localized path for crack growth.

Introduction

The growth of crack-like defects under the influence of residual stresses in AISI Type 316 weld metal at 538 C (1000 F) is a potential problem in high temperature structures. This paper describes an investigation of this problem and provides a displacement based analysis for comparison with other steels.

Creep Cracking in Type 316 Stainless Steel Welds

Notched bars of AISI 316 steel welds at 595 C (1103 F) were tested to creep rupture by Christoffel (Ref. 1). Results indicated that the material was 'notch strengthened' like the base metal at similar temperatures (Ref. 2). Material was defined as notch strengthened when its rupture life in a notched specimen exceeded that of a plain bar at the same stress level (net section stress compared with nominal stress on plain bar). For many years, notch strengthening was considered an adequate safeguard against failure by cracking.

Plain bars of Type 316 steel have been tested in a wide range of conditions and temperatures by Rowe and Stewart (Ref. 3) and Truman and Hardwicke (Ref. 4). Rupture ductilities were high (> 20% elongation), and the only data suggesting any problems with Type 316 weld metal were found in tests (Ref. 4) on welded pipes when longer times (> 5000 h) always produced failure in the weld metal. Unfortunately, there were no ductility data quoted.

Current Analyses of Creep Crack Growth

Notch strengthening effects are only applicable to purely tensile loading. The inherent strain gradients in bending can increase concentration effects at a notch. A recent approach (Refs. 5, 6) relies on the apparent values of elastic stress intensity in notched specimens subjected to combined bending and tension. Crack growth rate, dL/dt, was described by:

$$\frac{dL}{dt} = HK^{s}_{A} \tag{1}$$

where K_A is the calculated elastic stress intensity factor and H and s are constants for each material and temperature.

This linear elastic fracture mechanics approach has been used for the assessment of service cracking in low alloy steels (Ref. 7). The only published attempt to apply the method to stainless steels was by James (Ref. 8), who tested thin sheets of cold rolled 316 steel at 538 C (1000 F). The data showed good correlation between crack growth rate and stress intensity in two geometries of test piece. However, since the heat treatments and specimen thicknesses were not relevant to thick sections of welds, it is not possible to use the data in these situations.

It can be argued (Ref. 9) that linear elastic fracture mechanics is inappropriate to creep crack growth in many reported tests because it does not correctly describe displacements at a crack tip within a creeping specimen. Laboratory tests did not simulate the smaller crack opening displacements (COD) found in large components, and the data were likely to cause rejection of plate containing harmless cracks. Thus, although the approach is safe, improvements are desirable to avoid unnecessary repairs and outage times on equipment.

An alternative approach, describing crack growth in terms of crack tip displacements, was used (Ref. 10) to account correctly for the effects of creep deformation. Since COD is not easily measured in practice, a method for calculating appropriate reference stresses was proposed (Ref. 10) so that displacements and lifetimes might be calculated from plain bar creep data. This approach is based on slip-line field theory and is applicable to creep ductile materials (such as cast turbine steels) where creep deformation extends across the whole specimen. It does not account for the results of James (Ref. 8) where events near the crack tip control crack growth.

The COD approach predicted crack growth rates according to equation (2) for a range of Cr-Mo-V steels (Ref. 10):

$$\frac{dL}{dt} = A\left(\frac{d\delta}{dt}\right)^{0.8}, \text{ for } \delta \geq \delta_i \tag{2}$$

where δ is the COD, δ_i a critical COD for initiation of creep crack growth (Ref. 11) and A is a constant varying between one and eight for a range of tempered, fine grained Cr-Mo-V steels (Ref. 10). A linear relation between crack tip displacement and crack growth usually applies for time-independent plasticity (Ref. 12), so the index 0.8 in equation (2) quantifies embrittlement effects which operate only over extended periods. Mechanis-

J. R. HAIGH is with Central Electricity Research Laboratories, Leatherhead, Surrey, England

tically, the embrittlement results from a change to intergranular cracking in longer term tests on low alloy steels.

Experimental Procedure

Test Material

Material was obtained from a test weld which simulated a design of a particular cylindrical butt weld by use of appropriate restraint and choice of electrodes. There was no postweld heat treatment.

The creep crack growth tests were performed on the weld metal. Composition is shown in Table 1. The microstructure was a mixture of austenite and δ-ferrite and is discussed later.

Table 1—Composition of Type 316 Weld Metal (Wt. %)

Cr	Ni	Mo	C	Mn	P	S
18.2	11.3	2.3	0.04	0.80	0.011	0.010

Some creep data for material from the same weld are shown in Fig. 1. There is scatter inherent in the results because standard (small) creep specimens of 6.3 mm (0.248 in.) diameter only sampled one or two grains or weld beads.

Test Piece Design and Machining

T-type wedge opening loading specimens (WOL) 25 mm (1 in.) thick were machined to the dimensions shown in Fig. 2. The orientation of the machined notch to the grain directions varied among the tests as described later. The choice of 25 mm thick WOL specimens with side grooving was made to obtain the best possible simulation of a cracked weld subjected to residual (shrinkage) stresses which applied a bending moment. Also, plane strain conditions prevailed throughout much of the specimen section since side grooving suppressed most of the plane stress deformation associated with side surfaces near the crack.

The specimens were notched by spark machining 2 mm (0.079 in.) from the machined slot and then precracked a further 2 mm by fatigue at room temperature and a low stress intensity amplitude ($\Delta K \leq 20 MN \cdot m^{-3/2}$) ($\Delta K \leq 18.2$ ksi $\cdot in.^{1/2}$) in zero to tension loading. The maximum load during precracking was less than half of that used in the subsequent test. Fatigue cracks were intended to simulate the most severe defects possible in a service situation and proved to be similar in nature to the creep cracks discussed in the Section on Fractography and Metallography. Thus there was the minimum possible barrier to initiation of creep crack growth.

Creep Crack Growth Testing

The creep crack growth tests were at 538 C with static loads applied by a 50 kN (11,240 lbf) machine. Details of the furnace, temperature control and crack length monitoring were described earlier (Ref. 13), as were the loading procedure and displacement measurements (Ref. 10). Two displacements were obtained: (a) those along the loading line after application of the load, termed y, and (b) crack tip displacements (δ) derived from y by assuming rigid rotation about a hinge point in the uncracked ligament.

It can be shown (Ref. 10) that even quite substantial errors in predictions of hinge point positions cause only small (≤ 20%) inconsistencies in assessments of crack tip displacements. Thus the whole range of loading beyond the scope of linear elastic fracture mechanics can be assessed by such COD estimates with reasonable accuracy. Displacement readings (y) were consistent to ± 50 μm over a long period, equivalent to COD values of ~ ± 15 μm.

The increments in y during a test consisted of an inelastic (creep and plastic) component and elastic contribution since specimen compliance (reciprocal stiffness) increased with crack length. The average compliance change around L = 36 mm (1.42 in.) was taken to be 1.1 μm/kN/mm of crack growth (measured in earlier tests on steels at 550 C or 1112 F) and gave an elastic (reversible) contribution of 20 to 30% of y in the present tests.

Crack length readings by the electrical resistance technique were not so simple in the present material as in earlier work on creep ductile steels (Ref. 10) because crack tip displacements were much lower in the 316 weld metal. Thus electrical conduction across oxide and particularly the irregularities on the fracture surface caused spuriously low readings. It was assumed that the calibration was reduced in proportion to the crack growth, although in practice this probably underestimated crack growth in the early stages. A few checks were possible, after testing, by observation of the fracture surface. Accuracy was limited to ±0.2 mm (0.0079 in.) in tests 1 and 2 and was not obtainable in test 3. In the latter case, crack length was best inferred from changes in the elastic displacement (see below).

Details of the testing parameters are

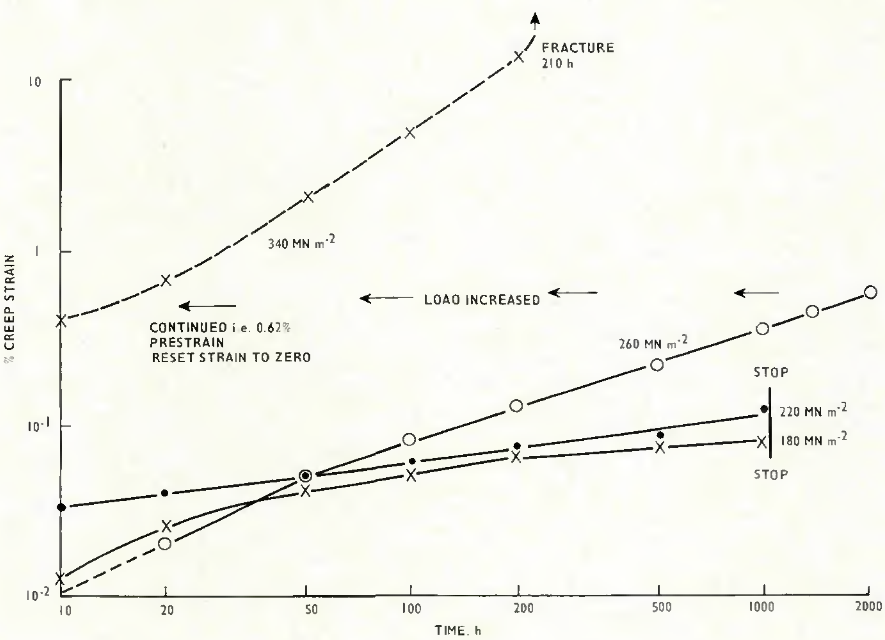

Fig. 1—Creep properties of Type 316 weld metal at 538 C (1000 F)

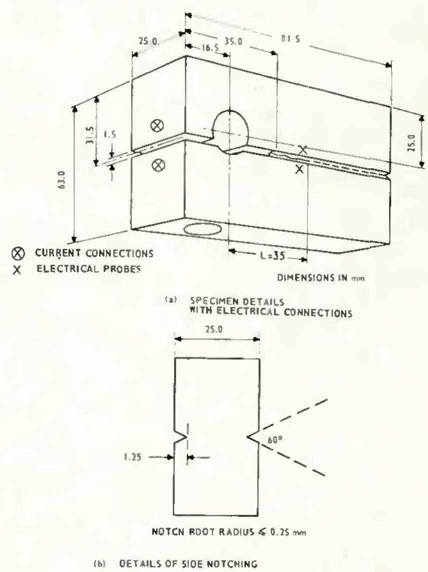

Fig. 2—Wedge opening loading (WOL) specimen details

listed in Table 2. The stress intensity and reference stress values (calculated as in Ref. 10) are nominal and represent the two extremes of available analytical techniques, applicable respectively to linear elastic and purely plastic deformation. Each test resulted in an appreciable permanent opening of the crack, but only to about 10% of the extent of earlier tests on very ductile Cr-Mo-V steels. COD is used to describe specimen behavior since simple elastic or plastic theories are not likely to be accurate here.

Grains of weld metal grow perpendicular to the fusion face during welding. A range of angles was sampled as shown in Table 2. The last test straddled two angles of grain in a region where the welding had been interrupted.

Table 2—Creep Crack Growth Tests

Test no.	Load, kN (kips)	Initial stress intensity, $MNm^{-3/2}$	Initial stress intensity, ksi $(in.)^{1/2}$	Reference stress, MNm^{-2}	Reference stress, (ksi)	Test time, h[a]	Angle of grains to notch, deg
1	21.6 (4.86)	42	38.2	148	(21.5)	1000	40
2	27.1 (6.09)	52	47.3	185	(26.8)	440	28
3	21.6 (4.86)	44	40.0	170	(24.7)	2400	14/35[b]

(a)All tests were discontinued before failure.
(b)Two stages.

Experimental Results and Discussion

Crack Growth and Displacements

Figures 3, 4 and 5 show the crack lengths (L) and displacements (y and δ) during the three tests. The displacements suggested that hardening occurred throughout the tests. The decline in displacement rates continued despite a rise in the general stress levels during continued crack growth. Elastic displacements were less than one third of the total changes during the tests. Thus the crack tip displacements were not related to elastic stress intensity factor, K. There is, therefore, no justification for using equation (1) to analyze the data for Type 316 weld metal. Similarly the reference stress levels were considerably different from the stresses used for the basic creep data (Fig. 1), hence the results will be expressed in terms of displacements. These data are only strictly applicable to the present geometry, and thus the results should not be extended to other loading conditions without testing the relevant geometry.

Crack growth began early in tests 1 and 2, so the critical COD for crack initiation was small ($\delta_i < 20\mu m$). The crack grew steadily throughout the tests with perhaps a slight decline in test 1 as the creep displacement rate decreased.

Test 3 (Fig. 5) was exceptional even though the creep rates were similar to test 1 (as expected at similar load and crack length). Crack growth was slower (almost by a factor 10) up to 2230 h when there was a sharp increase in crack length and displacement. Clearly the new displacement was elastic in nature and corresponded to the 2 mm of crack growth observed in a microsection (see Section following).

Figure 6 shows crack growth rates as a function of the combined elastic and creep displacements at the initial crack tip region. (In test 3 rates were averaged to include the 'jump' in the crack growth). Results are compared in Fig. 6 with those obtained earlier (Ref. 10) for low alloy steels since these are the only directly comparable (same specimen geometry) data points available at present. These earlier results, denoted by solid lines, represent a power relation with index less than unity in equation (2). The results for the tempered bainite steel can be extrapolated downwards to give similar rates to those of the Type 316 weld metal. Alternatively, the aspect ratios (crack growth rate/crack opening rate at the crack tip and denoted by oblique dotted lines in Fig. 6) are higher in Type 316 weld metal than for the low alloy steels. The most severe aspect ratio (~ 230) was found in test 1.

The tempered bainitic 1%Cr-Mo-V steel represented a microstructure in a mildly heat-affected zone. Much more brittle behavior associated with low alloy steel welds can be inferred from results for severely quenched and

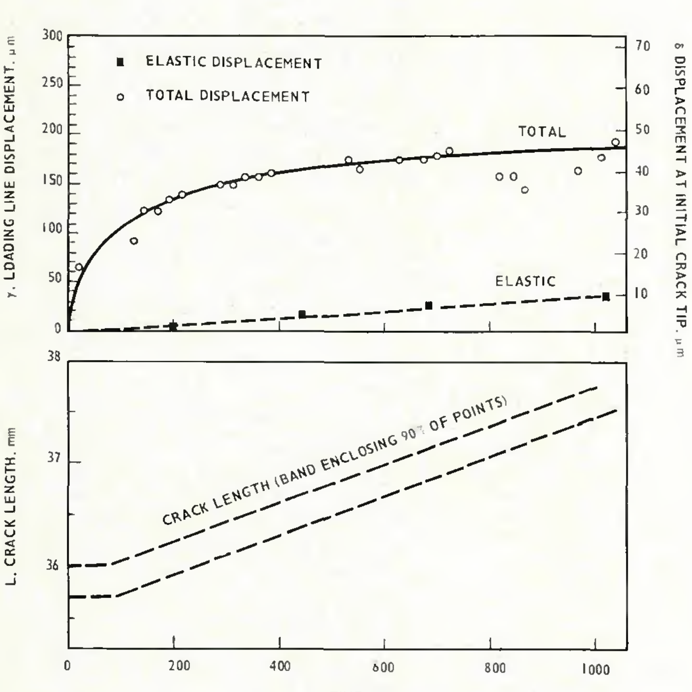

Fig. 3—Basic data from test 1 under 21.6 kN (4856 lbf) load

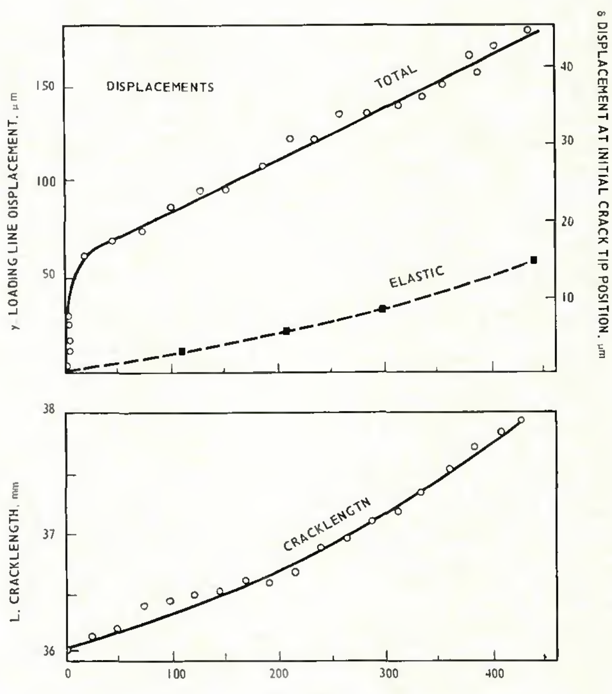

Fig. 4—Basic data from test 2 under 27.1 kN (6092 lbf) load

untempered ½%Cr-Mo-V steels (Ref. 6). Thus the Type 316 weld metal presents less severe cracking problems than some heat-affected zones in low

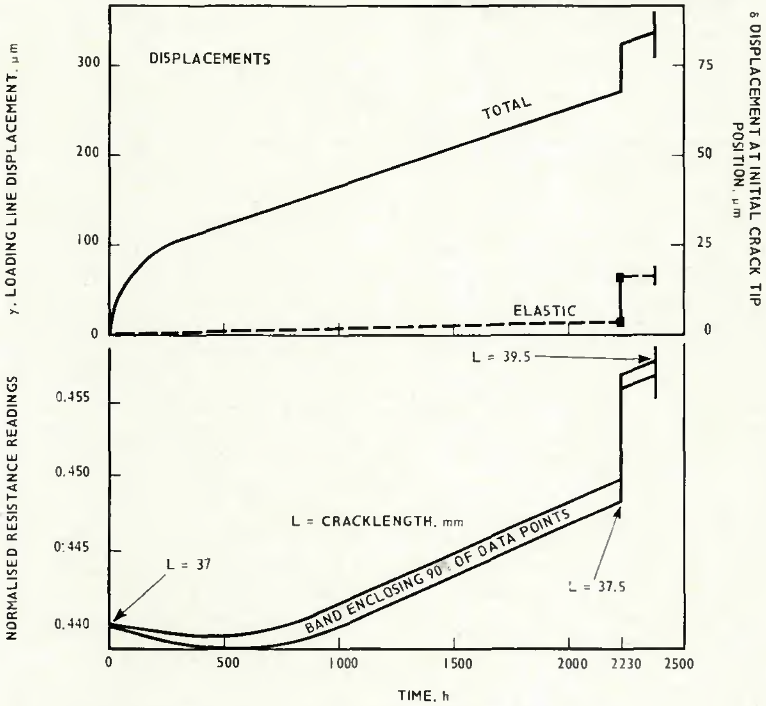

Fig. 5—Basic data from test 3 under 21.6 kN (4856 lbf) load

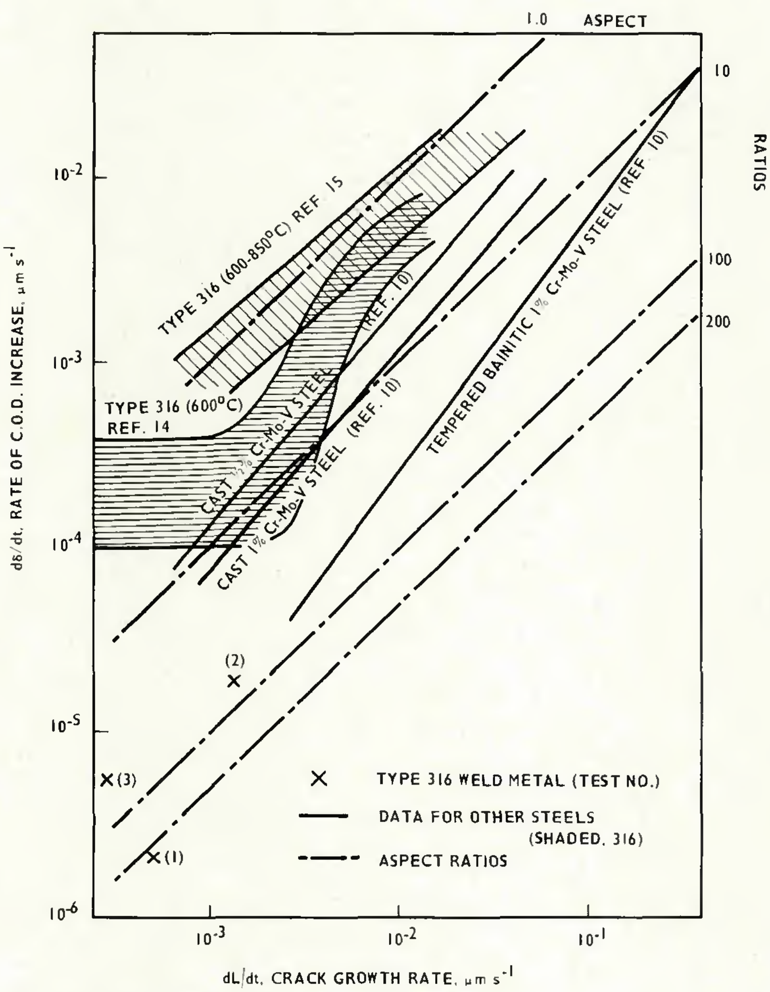

Fig. 6—Crack growth rates as a function of COD increase

alloy steels.

Other recent data (Refs. 14, 15) on 316 steels are shown in Fig. 6. Williams' data (Ref. 14) are for specimens of comparable thickness to the present work and which bend during testing. As in Ref. 15 the temperature was 600 C (1112 F), but in the latter case much thinner (0.78 mm) (0.031 in.) specimens were used. These appeared much more ductile than the thicker samples of base metal examined in Ref. 14. The relevance of small notched specimens in the assessment of thick components is thus very questionable and explains why notch-rupture tests failed to show the weakness obtainable in the weld metal (Ref. 1). It is, however, apparent by examination of Fig. 6 that the base metal is more ductile than the weld metal.

Fractography and Metallography

Crack growth occurred with very little lateral contraction of the specimen (e.g., see Fig. 7). The fracture surfaces were normal to the side surfaces of the specimens. This usually implies plane stress deformation. Crack fronts were somewhat irregular in appearance but showed little tendency to bow up the center of the specimen (Fig. 7). This indicates a uniform degree of constraint through much of the specimen thickness. Thus the transfer of data to a thicker section of welds can be made with confidence. The quoted crack lengths are the maximum values along the irregular crack fronts.

The cracks grew in segregated regions of δ-ferrite within a matrix of austenite (Fig. 8). The localization of the crack path explained the brittleness of the material. Even the fatigue precrack grown at 25 C (77 F) followed δ-ferrite regions so that the creep and fatigue surfaces looked quite similar in the scanning electron microscope.

Cracking appeared to occur steadily with displacement throughout most of tests 1 and 2, but in test 3 was delayed by the boundary between weld beads where a change of grain orientation had also occurred. The delay appears to have ended only when the crack broke forward through the whole of the adjacent bead. A section is shown in Fig. 9 where the crack apparently began to re-initiate ahead of the obstacle but a more favorable path in a parallel plane allowed complete separation of the weld bead and caused some transverse fracturing parallel to the bead boundary. The delay at the bead boundary, which extended over most of the specimen thickness, was caused by lack of continuity of the δ-ferrite. An up-to-date review of δ-ferrite in austenitic welds was published recently (Ref. 16), and its role in creep failure has been observed in tensile creep tests at 650 C (1202 F) (Ref. 17).

Actually, the opening at the initial crack tip (δ_0) after unloading showed a permanent deformation (40 μm) plus 10 μm generated by reversible (elastic) loading of the whole specimen. This agrees fairly well with the value of 70 μm predicted from the displacement data of Fig. 5.

Fig. 7—Fracture surface of specimen 2. (×4, reduced 57% upon reproduction)

Fig. 8—Cracking in test 1. Etched in Vitella's reagent. ×300 (reduced 50% upon reproduction)

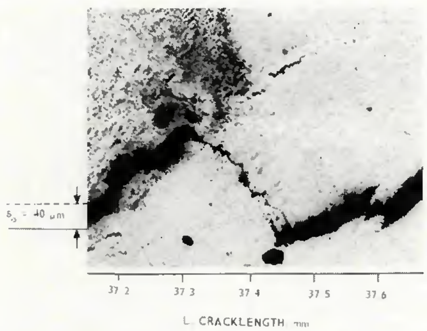

Fig. 9—Point of crack reinitiation (L = 37.3 mm) in test 3. Ferric chloride etch. ×210 (reduced 58% upon reproduction)

Discussion

It is clear that cracking can best be avoided by eliminating the occurrence of continuous δ-ferrite. This may be achieved by heat treatment after welding (Ref. 16), by keeping the δ-ferrite below about 4% (Ref. 16) or by obtaining small weld beads to use their boundaries as barriers. In cases where heat treatment is not possible, the use of small diameter electrodes may be desirable. Control of composition to eliminate δ-ferrite is not advisable as it can lead to solidification cracking in austenitic welds (Ref. 18).

Conclusions

Type 316 weld metal cracks more readily at 538 C than wrought materials and may therefore be prone to creep cracking under the influence of residual stresses in unrelieved welds. Displacement changes due to creep at 538 C in deeply notched specimens subjected to bending moments were at least twice those expected from elastic loading, and hence a linear elastic fracture mechanics approach to creep crack growth in this material is not recommended. An approach using displacements directly or calculating them indirectly by a suitable stress approach is required. Cracking problems are likely to be less severe when weld beads are small; thus the use of small diameter filler metal is justified.

Acknowledgments

Thanks are due to Mr. G. Willoughby for providing testing facilities and Dr. J. A. Williams and Mr. R. Nicholson (Refs. 14, 15) for providing unpublished data. The work was carried out at the Central Electricity Research Laboratories and the paper is published by permission of the Central Electricity Generating Board.

References

1. Christoffel, R. J., "Notch Sensitivity of the Heat-Affected Zone in Type 316 Material," *Welding Journal,* 42 (1), Jan. 1963, Res. Suppl., pp. 25-s to 28-s.

2. Garofalo, F., "Creep Rupture Behaviour of Notched and Unnotched Specimens of Types 304, 316 and 321 Austenitic Stainless Steels," Proceedings ASTM 59, 1959, pp. 957-972.

3. Rowe, G. H., and Stewart, J. R., "Creep Rupture Behavior of Type 316 Stainless Steel Weldments Prepared with and without Restraint," *Welding Journal,* 41 (12), Dec. 1962, Res. Suppl., pp. 534-s to 541-s.

4. Truman, R. J., and Hardwicke, D., "Some Effects of Heat Treatment and Welding on the Rupture Properties of Three Austenitic Steels," in "High Temperature steels," The Iron and Steel Institute, London, 1967.

5. Siverns, M. J., and Price, A. T., "Crack Growth under Creep Conditions," Nature, 228, 1970, pp. 760-761.

6. Neate, G. J., and Siverns, M. J., "The Application of Fracture Mechanics to Creep Crack Growth," Paper 234/73 in "Creep and Fatigue in Elevated Temperature Applications", Instn. Mech. Engrs., London, 1974.

7. Oates, G., "The Application of Non-Destructive Testing Techniques to Welds in Creep Resisting Steels," in "Welding Creep Resistant Steels," Welding Institute, Abington, U.K., 1975 (Jan.).

8. James, L. A., "Some Preliminary Observations on the Extension of Cracks under Static Loading at Elevated Temperatures," Int. J. Fracture Mechanics, 8, 1972, pp. 347-349.

9. Haigh, J. R., and Richards, C. E., "Limits in the Application of Fracture Mechanics to High Temperature Fatigue Crack Propagation in a Turbine Steel," Paper 159/73 as in Ref. 6.

10. Haigh, J. R., "The Mechanisms of Macroscopic High Temperature Crack Growth," Materials Science and Engineering, 1975, 20 (3), pp. 213-35.

11. Wells, A. A., and McBride, F. H., "Application of Fracture Mechanics to High-Temperature Creep Rupture," Canadian Metallurgical Quarterly, 6 (4), 1967, pp. 347-368.

12. McClintock, F. A., "On Notch Sensitivity," *Welding Journal,* 40 (5), May 1961, Res. Suppl., pp. 202-s to 209-s.

13. Haigh, J. R., "The Growth of Fatigue Cracks at High Temperatures under Predominantly Elastic Loading," Engineering Fracture Mechanics, 1975, 7, pp. 271-284.

14. Williams, J. A., private communication, C.E.G.B. Marchwood Engineering Laboratories, Southampton, U.K.

15. Nicholson, R., private communication, C.E.G.B. Berkeley Nuclear Laboratories, Gloucestershire, U.K.

16. Delong, W. T., "Ferrite in Austenitic Stainless Steel Weld Metal," *Welding Journal,* 53 (7), July 1974, Res. Suppl., pp. 273-s to 286-s.

17. Goodwin, G. M., Cole, N. C., and Slaughter, G. M., "A Study of Ferrite Morphology in Austenitic Stainless Steel Weldments," *Welding Journal,* 51 (9), Sept. 1972, Res. Suppl., pp. 425-s to 429-s.

18. Hull, F. C., "Effect of Delta Ferrite on the Hot Cracking of Stainless Steel," *Welding Journal,* 46 (9), Sept. 1967, Res. Suppl., pp. 399-s to 409-s.